

HUMAN BODY DETECTION TECHNOLOGY BY THERMOELECTRIC INFRARED IMAGING SENSOR

Masaki Hirota
Yasushi Nakajima
Masanori Saito
Makoto Uchiyama
Nissan Motor Co., LTD
Japan
Paper Number 207

ABSTRACT

This paper describes a newly developed thermoelectric infrared imaging sensor, having a 48 x 32 element thermoelectric focal plane array (FPA), and two experimental vehicle systems. One is a blind spot pedestrian warning system that employs four infrared imaging sensors. This system helps alert the driver to the presence of a pedestrian in a blind spot by detecting the infrared radiation emitted from the person's body. The system can also prevent the vehicle from moving in the direction of the pedestrian. The other is a rearview camera system with an infrared detection function. This system consists of a visible camera and infrared sensors, and it helps alert the driver to the presence of a pedestrian in a rear blind spot. The FPA is basically fabricated with a conventional IC process and has the potential for low cost.

INTRODUCTION

Advances in electronics in recent years have led to the adoption of many different types of sensors on vehicles, including pressure sensors, accelerometers and visible charge-coupled device (CCD) cameras. These devices are being used to meet societal demands for cleaner exhaust emissions, lower fuel consumption and help improve safety and comfort, among other requirements. In Japan, safety performance of vehicles has been a rising concern in conjunction with the increase in traffic accident fatalities since the late 1980s.

Infrared (IR) radiation refers to a form of light having wavelengths longer than those of visible light. Various types of warm bodies, including the human body, emit IR radiation or visible light corresponding to their temperature. Infrared sensors capable of detecting such radiated energy are an extremely useful means of human body detection because they can detect the

presence of a person even at night without any illumination.

The IR radiation emitted by the human body, however, is of the long wavelength type (LWIR) in the 10- μ m wavelength band, and its detection requires some ingenuity because of its extremely low energy level compared with that of visible light. Detection methods until the 1980s were limited to the use of cooled sensors (HgCdTe detectors, etc.) that were cooled to ultra-low temperatures in the vicinity of 77 K. Such sensors could not be used on ordinary passenger cars because of such aspects as the cooling system service life, weight and power consumption.

However, two types of uncooled IR imaging sensor, which had been originally developed as a U.S. military technology^(1,2), were implemented in commercial applications in 1992. These sensors provide detection performance nearly equal to that of cooled devices. The IR focal plane array (IR-FPA) used in these uncooled IR imaging sensors requires accurate temperature control in the vicinity of the phase transition temperature, necessitating the use of an additional device such as a Peltier thermoelectric cooler. Even uncooled IR imaging sensors, which have fewer components than cooled IR imagers, are still high in cost, which limits their automotive use to high-end luxury cars at present. To promote widespread use of IR imaging sensors on vehicles in the coming years, it is necessary to reduce their cost further. We have focused on the thermoelectric type of IR-FPA^(3,4,5) that is highly compatible with the conventional IC manufacturing process, does not require any temperature control mechanism or optical chopper and allows easy design of the second-stage processing circuit because of its thermoelectric nature, all of which help to give it a low cost potential. A CCD type of thermoelectric IR-FPA with over 10,000 pixels has already been announced.⁽³⁾ However, we adopted a CMOS imager system⁽⁵⁾ with the aim of reducing the cost further, and have attained

high sensor performance by miniaturizing and optimizing the thermoelectric IR-FPA.

Moreover, we have applied the thermoelectric IR imaging sensor research to develop a prototype nighttime pedestrian warning system⁽⁶⁾ and a blind spot pedestrian warning system. These systems were developed through our participation in the first and second phases of the Advanced Safety Vehicle (ASV) project promoted by the Ministry of Transport (currently the Ministry of Land, Infrastructure and Transport) beginning from 1991.

This paper describes the thermoelectric IR imaging sensor, the blind spot pedestrian warning system research incorporated in the Nissan ASV-II and a rearview camera system with an IR detection function.

INFRARED IMAGE SENSOR

Infrared Radiation Emitted by Human Body

Infrared radiation is a form of electromagnetic radiation having wavelengths from 0.78 to 1,000 μm and is one type of light wave. With respect to IR applications, the bandwidths having high transmittance in the atmosphere (atmospheric window) are divided into the short wavelength IR (SWIR) region, middle wavelength IR (MWIR) region and long wavelength IR (LWIR) region, as shown in Fig. 1. Selective use is made of these different wavelength regions depending on the target temperature.

The wavelength characteristics of the IR radiation emitted by the human body are determined by its radiant exitance, which is determined by the absolute temperature of the human body surface and its emissivity.

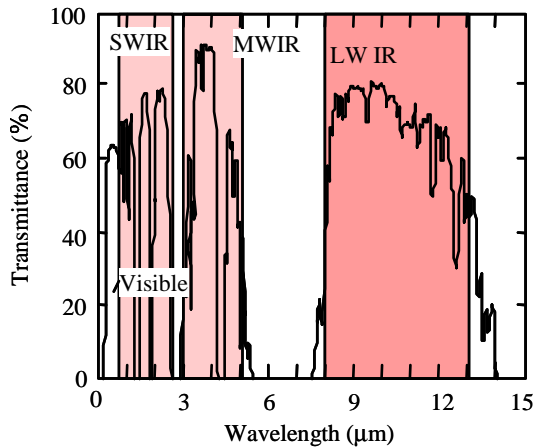


Fig. 1 Spectral transmittance characteristics in the atmosphere

As the first step of this study, the atmospheric temperature dependence of the facial surface temperature and the influence of solar radiation were measured in an environmental testing facility for automobiles. Under a shady condition, with only illumination and air-conditioning ventilation, the facial surface temperature showed a very small change of 4.1°C in relation to an atmospheric temperature change of 30°C, as shown in Fig. 2. Even under a condition of midsummer solar radiation (height of the illumination used for solar radiation was 3 m and the energy density at the floor was 2.76 MJ/m² x h), it was found that the facial surface temperature rose only 1°C compared with that under the shady condition. At an atmospheric temperature of 27°C (300K) or lower, it was observed that a temperature difference of 5°C or more was obtained with respect to the facial surface temperature.

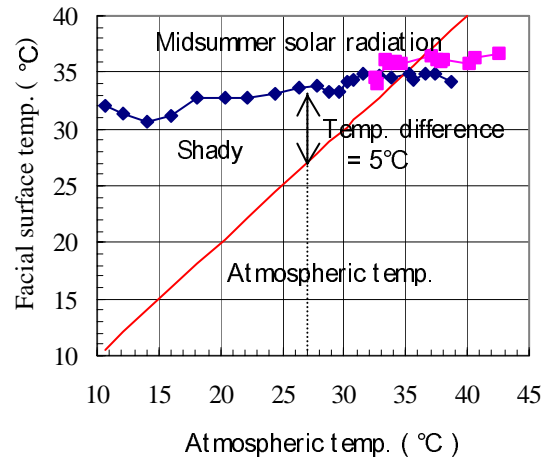


Fig. 2 Dependence of facial surface temperature on atmospheric temperature and solar radiation (height of the face: 1.7 m; air-conditioning ventilation only; height of illumination used for solar radiation: 3 m; solar energy density: 2.76 MJ/m² x h)

The characteristics of IR radiation emitted by the human body were then determined. An object that absorbs all light is referred to as a blackbody, and it also becomes a complete radiator under the application of Kirchhoff's law. The emissivity of the human body is around 0.98, which is close to that of a blackbody. The spectral radiant exitance of a blackbody is determined by Planck's radiation law and is given by

$$W_{\lambda} = 2 \pi h c^2 / [\lambda^5 (e^{hc/\lambda kT} - 1)] \quad (1)$$

where W_{λ} is the emitted radiation per unit wavelength and unit area (W/cm² x μm), h is Planck's constant (= 6.63 x 10⁻³⁴ W x s²), k is the Boltzmann constant (= 1.38 x 10⁻²³ W x s/K) and T is the absolute temperature (K).

The maximum radiation intensity wavelength λ_m can be found with Wien's displacement law as

$$\lambda_m \times T = 2.897 \pm 0.4 \mu\text{m} \times \text{K} \quad (2)$$

As is clear from Fig. 2, the facial surface temperature is nearly constant in a range of 31°-36°C (304-309K). Therefore, the maximum radiation intensity wavelength of the IR radiation emitted by the human body is $\lambda_m \approx 9.5 \mu\text{m}$, as indicated in Fig. 3. Accordingly, use of LWIR radiation in a wavelength range of 8-13 μm is suitable for human body detection.

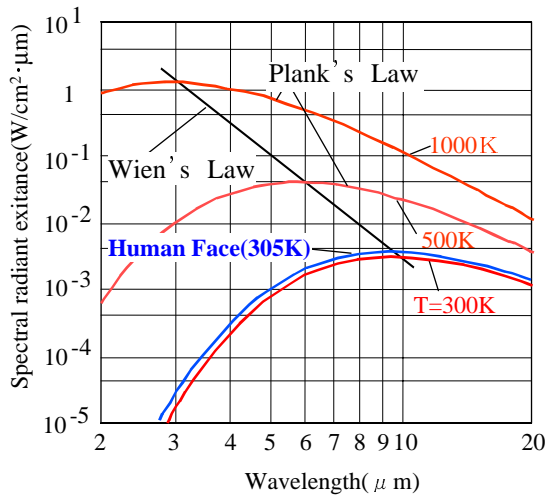


Fig. 3 Spectral radiant exitance of a blackbody

48x32 element Thermoelectric IR FPA

The thermoelectric IR-FRP consists of tiny thermocouples connected in series that utilize the Seebeck effect to convert the temperature difference between the hot and cold junctions into a voltage. In order to increase the temperature difference, the thermocouples are formed on a thin membrane that is fabricated in a micromachining process. The thermocouples are fabricated of p-type and n-type polysilicon layers, consisting of materials commonly used in general semiconductor processes and connected in series.

Figure 4 shows the sensor structure of one pixel of a prototype 48 x 32 element thermoelectric IR-FPA. Incident IR radiation is absorbed by the Au-black absorber in the center of the sensor and converted to thermal energy, which is transmitted in turn via the hot junctions, beam and cold junctions by means of heat radiation to the Si substrate that serves as a heat sink. To increase the thermal resistance between the hot and cold junctions, a portion of the Si substrate is removed to form a cavity. In addition, high sensitivity is attained by using a vacuum-sealed package to avoid internal

heat conduction through the air. The responsivity R of the thermoelectric IR-FPA is given by

$$R = n \cdot \alpha \cdot R_{th} \cdot \eta \quad (3)$$

where n is the number of thermopile pairs, α is the Seebeck coefficient (sum of p-type and n-type), R_{th} is the thermal resistance between the hot and cold junctions and η is infrared absorptivity. Equation (3) indicates that increasing η and R_{th} is effective in improving responsivity R. The optimum values of η and R_{th} were calculated on the basis of the sensor size and the accuracy of the fabrication process. Additionally, a precisely-patterned, high-IR absorptivity Au-black layer, which was developed independently in our laboratories, was adopted to improve η . As a result, absorptivity of more than 90% has been achieved at a wavelength of 10 μm .

This pixel structure was then used to fabricate the prototype 48 x 32 element thermoelectric IR-FPA. A scanning electron micrograph of the 48 x 32 element IR-FPA chip is shown in Fig. 5. The dimensions of the various parts of the sensor are as follows: chip size of 10.5 x 7.44 mm, pixel pitch of 190 x 190 μm and thermopile width of 0.8 μm for the six pairs of thermopiles. The positive terminal of each pixel is connected to an output line through two built-in NMOS transistors controlled by an external input signal. The negative terminal of all the pixels is connected to the same common terminal. Additionally, because this device has comparatively high internal resistance of 116 k Ω , it is necessary to limit the bandwidth of the second-stage circuit for the purpose of reducing Johnson noise (thermal noise). In order to obtain the desired video frame rate, the entire sensor is divided into 12 blocks of four columns each, and signals are output in parallel from 12 output lines. This vacuum-sealed IR-FPA achieves responsivity of $R = 21,000 \text{ V/W}$ and a thermal time constant of 25 msec, representing high levels of performance compared with similar commercial devices.

This thermoelectric IR-FPA with its low cost potential was then incorporated into an IR imaging sensor that has been developed independently in our laboratories for automotive applications. A photograph of the IR imaging sensor is shown in Fig. 6, and its specifications are given in Table 1. The IR imaging sensor is a compact, lightweight device, measuring 100 mm in width, 60 mm in height (excluding the bracket) and 80 mm in depth and weighing 400 g.

A block diagram of the IR imaging sensor is shown in Fig. 7. The sensor has a germanium meniscus single-element lens with a focal length of $f = 15 \text{ mm}$ and $f/0.7$. Both sides of the lens are coated with an anti-reflection coating having a wavelength of 10 μm .

This IR imaging sensor operates under a program stored in a Read Only Memory (ROM) incorporated in the Central Processing Unit (CPU, SH7034). The 2-D array sensor outputs successive signals in parallel from the 12 blocks based on an address signal request from the CPU. The output signals are amplified and sent to the CPU via an 8-bit analog-to-digital converter (ADC). The CPU performs offset compensation and responsivity compensation and then makes a pedestrian detection judgment. A function is also included for converting video data to an NTSC video signal by means of a video digital-to-analog converter (DAC). This IR imaging sensor can output a pedestrian detection signal and image data in the NTSC video signal format via the RS-232C interface. With its f/0.7 lens, the IR imaging sensor achieves a noise equivalent temperature deviation (NETD) of less than 0.4°C.

Figure 8 shows a facial image of a person wearing eye glasses that was obtained with this IR imaging sensor. The eye glasses portion appears as a dark region because infrared rays in the 10- μm wavelength band do not pass through glass.

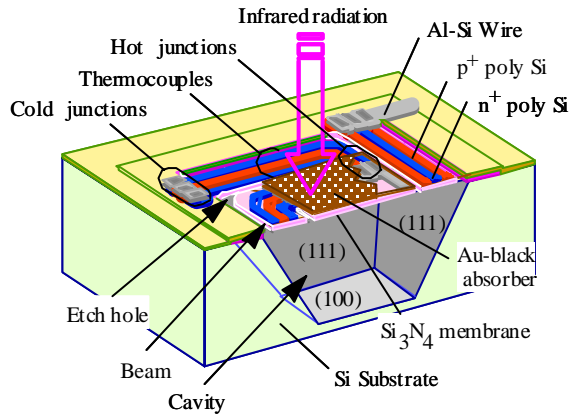


Fig. 4 Sensor structure of one pixel of the 48 x 32 element thermoelectric IR-FPA

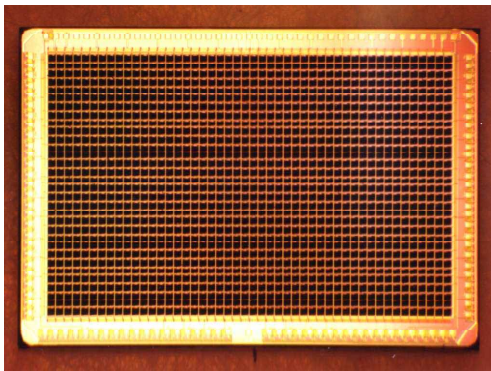


Fig. 5 SEM micrograph of the 48 x 32 element thermoelectric IR-FPA (chip size: 10 x 7.44 mm)



Fig. 6 Automotive IR imaging sensor incorporating the 48 x 32 element thermoelectric IR-FPA

Table 1 Specifications of the IR imaging sensor

Performance Parameter	Capability (@300K)
Array configuration	48 x 32
Chip dimensions	10.5 mm x 7.44 mm
Pixel size	190 μm
Spectral response	8 – 13 μm
Responsivity	2100 V/W
Thermal time constant	25 msec
Lens	f = 15 mm, f/0.7
NETD (@f0.7)	0.4 °C
Field of view	30° x 20°
Outputs	RS-232C, Detection, NTSC
Power	12 V, 0.25 A
Overall dimensions	100 mm x 60 mm x 80 mm
Weight	400 g

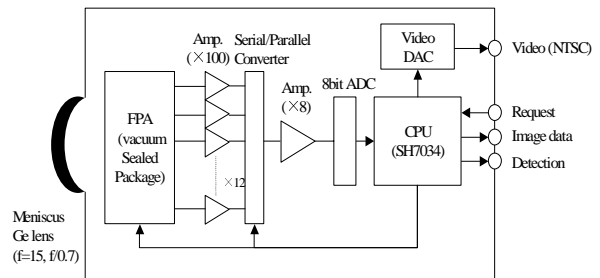


Fig. 7 Block diagram of the automotive IR imaging sensor

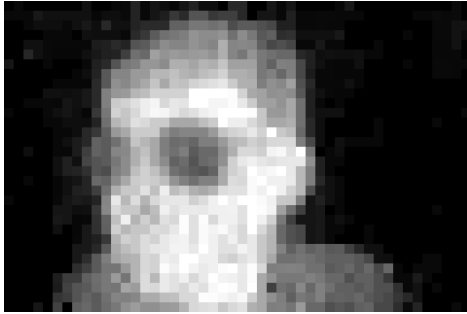


Fig. 8 IR image obtained with the automotive IR imaging sensor

BLIND SPOT PEDESTRIAN DETECTION SYSTEM RESEARCH

Concept

This system was incorporated in the Nissan ASV-2. The concept of this system is to detect infrared radiation emitted by the human body or other objects with the aim of helping to prevent blind spot accidents by alerting the driver to be careful and by preventing the vehicle from moving in the direction of a detected person. This is accomplished by four IR imaging sensors, mounted at the front and rear, which detect children or other heat sources in the driver's blind spots (within 3 m and within the sensor field of view) where they cannot be seen and could become obstacles as the vehicle begins to move. The concept of the system is illustrated in Fig. 9.

Two new functions were added to this system, taking into account the characteristics of blind spot accidents. One is a human body detection function using four IR imaging sensors, and the other is a function for preventing the vehicle from moving by means of braking control. There can be a time difference ranging from several seconds to several minutes between the time a driver enters a vehicle and starts the engine and the time the vehicle is put in motion. It is possible that the circumstances around the vehicle may change during that interval. Because children in particular are apt to do unexpected things, incidents have been reported where blind spot accidents occurred even though the driver confirmed the safety of the environment around the vehicle before getting in. The IR imaging sensors, capable of detecting IR radiation emitted by the human body regardless of whether it is day and night, were adopted for this system because it was thought that a function for selectively detecting the human body and other heat sources would be the best way of helping to prevent such blind spot accidents. The function for preventing vehicle movement by braking control was added as a

capability because there are instances when there is insufficient time to execute an evasive maneuver because of the extremely short distance between a vehicle and an obstacle.

System Configuration

The system configuration is shown in Fig. 10. Infrared imaging sensors mounted at the vehicle's four corners serve to detect a pedestrian in the driver's blind spots. In the event a pedestrian is present in the direction in which the vehicle is about to move, the system issues audible and visual warnings to alert the driver and activates throttle and brake actuators to prevent the vehicle from moving. The components making up the system include: four IR imaging sensors incorporating a pedestrian detection judgment capability; a blind spot pedestrian warning control unit that integrates the signals from the IR imaging sensors and sends a signal to the Control Area Network (CAN); a vehicle motion control unit or an Auto Box (main controller) that manages vehicle motions; an integrated human-machine interface (HMI) control unit; a monitor and a warning unit; and throttle and brake actuators that prevent the vehicle from starting off.

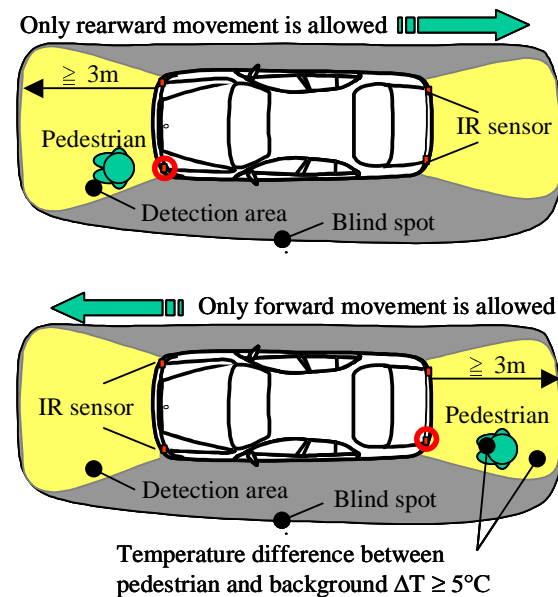


Fig. 9 Concept of the blind spot pedestrian warning system

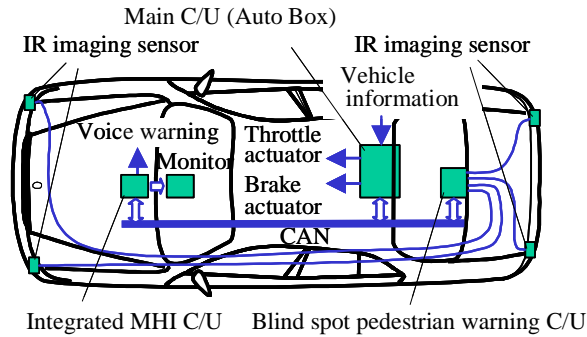


Fig. 10 Overview of the blind spot pedestrian warning system

Detection Range of IR Image Sensor and Mount Position

The mounting positions of the IR imaging sensors are closely related to their detection range. A study was made of the mounting positions under the following conditions.

- (1) Two IR imaging sensors each would be used at the front and rear, for a total of four sensors.
- (2) The sensors would have a field of view of 30° (horizontal) by 20° (vertical).
- (3) The detection range would be 3 m under the condition that the temperature difference $\Delta T = T_t - T_e = 5^\circ\text{C}$.
- (4) The sensors would be mounted so that they did not interfere with the lamps, cooling equipment, tailpipe and other vehicle parts.

An experiment was conducted to measure the potential blind spot areas around the Nissan Cima (FY33) sedan that was the base vehicle of the Nissan ASV-2. The eye point in the driver's seat was set at a height of 1.05 m from the ground. Measurements were made of the areas where the ground (ground height of 0 m) could not be seen directly with the eye or by means of the mirrors from the driver's seat, assuming that the task was to detect a human body lying on the ground. The results are shown in Fig. 11. It was found that the blind spots at the front were within a distance of 2.7-4 m from the vehicle body and those at the rear were within a distance of 9-11 m. Taking those results into account, the positions of the four IR imaging sensors were determined so that they satisfied the four conditions mentioned above.

Photographs of the test vehicle are shown in Fig. 12. In Fig. 12-(b), two IR imaging sensors of the same type as those used at the front are mounted inside a germanium window at the rear. As indicated in Fig. 12-(a) and (b), the two front sensors were installed at a height of 370 mm and were spaced 1,580 mm apart, and

the two rear sensors were mounted at a height of 515 mm and were spaced 1,000 mm apart. The sensors at both the front and rear were positioned so that their optical axis was horizontal. The front sensors were installed at a relatively low height on account of the shorter blind spot distance at the front, while those at the rear were mounted higher because of the longer blind spot distance in the rearward direction and also to avoid interference with the tailpipe. The front sensors were spaced farther apart because a larger detection range was needed at the front than at the rear in connection with the front-wheel steering of the vehicle. The front and rear detection ranges thus determined for the system are indicated in Fig. 11-(b). With the present system, there are small areas very close to the front and rear of the vehicle where detection is not provided. To cover these areas as well, either the field of view would have to be expanded or approximately three sensors each would have to be installed at both the front and rear.

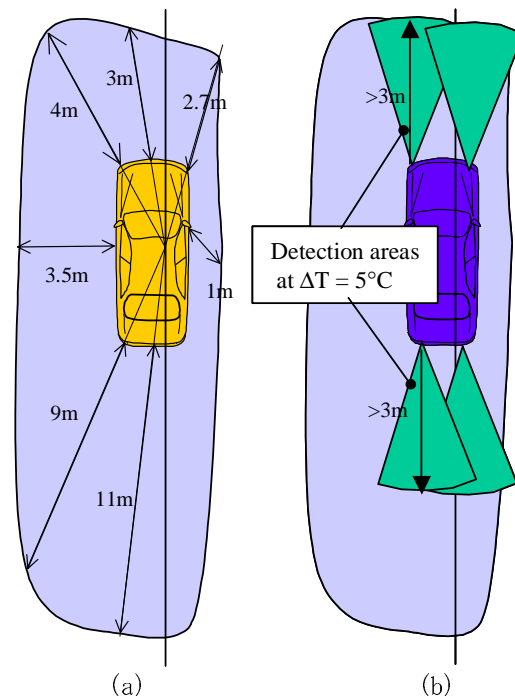


Fig. 11 (a) Road surface areas that cannot be seen from the driver's seat of the Nissan ASV-2 base vehicle (Cima) at an eye point height of 1.05 m from the ground and (b) detection areas at $\Delta T = 5^\circ\text{C}$

Operation

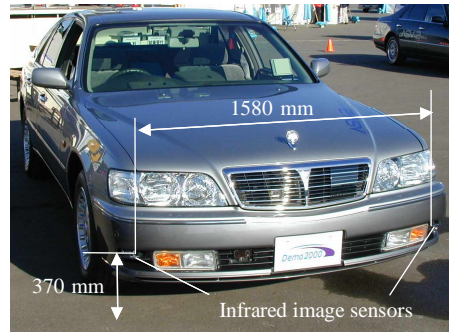
The flowchart in Fig. 13 outlines the operational sequence of the system. At the time the vehicle is stopped, it is assumed that there are no pedestrians in

the front and rear detection ranges. In response to a request signal from the Auto Box, the IR imaging sensors capture baseline image data (image A) and record the data in their internal memory units. When a vehicle is parked for a long time, it is presumed that the atmospheric temperature and sunlight will change, so the baseline video data (image A) are updated accordingly. The IR imaging sensors take images at periodic intervals of approximately 30 s and update the baseline image data (image A) if there is no heat source in the image. The baseline image data are not updated when a heat source is present.

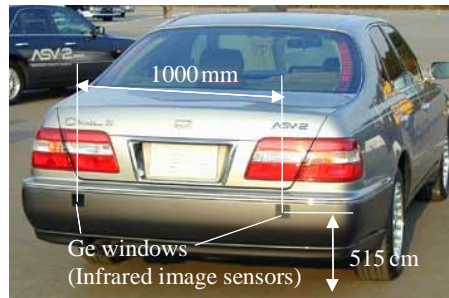
Also, at the time the vehicle is about to start off, the IR imaging sensors capture start-off image data (image B) in response to a request signal sent from the Auto Box. To remove the influence of background heat sources, a differential image (image C) is calculated by subtracting image A from image B. The IR imaging sensors then process differential image C to detect heat sources. When a heat source is detected, a detection signal and the position of the sensor that detected the heat source (e.g., right front) are sent to the Auto Box via the blind spot pedestrian warning control unit. If the position of the sensor that detected the heat source (i.e., front or rear) coincides with the vehicle's intended direction of movement, the Auto Box judges that a pedestrian is present in that direction. It then alerts the driver by means of an audible warning and a display screen indicator, using signals sent through the integrated HMI control unit.

The Auto Box also activates brake and throttle actuators that forcibly prevent the vehicle from moving in the direction of the detected pedestrian. Conversely, if the sensor position and direction of movement do not coincide, the Auto Box judges that there is no pedestrian in the vehicle's direction of movement and allows the vehicle to proceed.

The system judges that a heat source is present if an object corresponding to a temperature difference of 4°C or greater is in 10 or more pixels of the above-mentioned differential image C. That number of pixels is approximately equal to the size of a human face at a distance of 3 m (corresponding to a 15-cm angle).



(a)



(b)



(c)

Fig. 12 Nissan ASV-2 equipped with the blind spot pedestrian warning system. (a) Front view, (b) rear view (with Ge window) and (c) enlarged front view

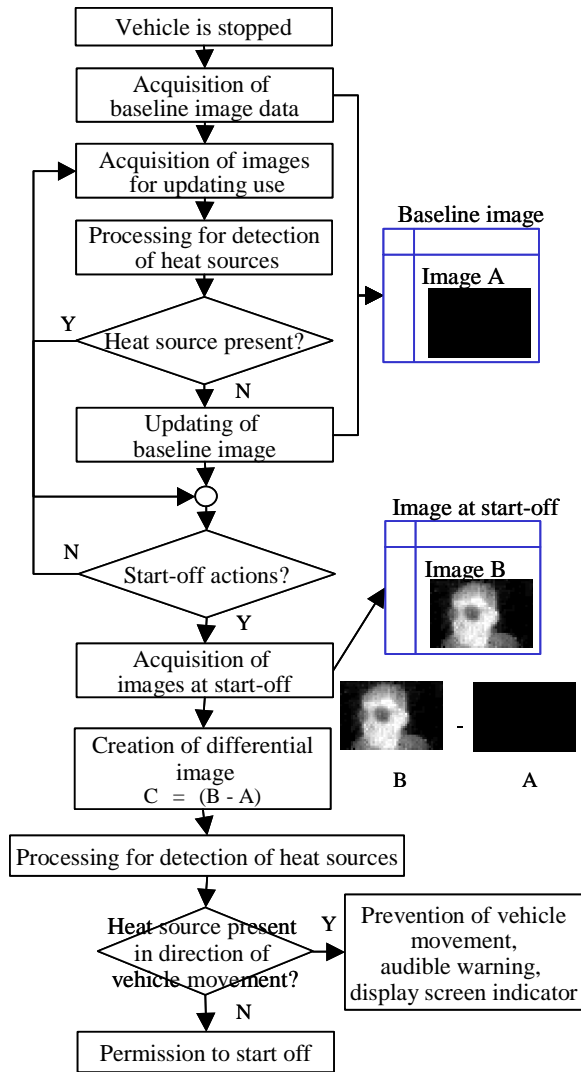


Fig. 13 Operational sequence of the blind spot pedestrian warning system

Detection Results

Human body detection distances were measured under different atmospheric temperature conditions to verify the operation of the prototype system. The results are given in Fig. 14. In a low temperature range of 10°-22°, the detection distance was 6-8 m, which would cover a large portion of the rearward blind spot mentioned in figure 11. On the other hand, the detection distance decreased to 3-3.5 m in a temperature range of 24°-30°C. Under a condition of a temperature difference $\Delta T = T_t$ (surface temperature of a pedestrian) - T_e (background temperature) $\geq 5^\circ\text{C}$ (i.e., the atmospheric temperature (background temperature) is no more than 27°C), a detection distance of 3 m or greater was obtained with

the prototype system specifications. Additionally, it was also confirmed in actual vehicle tests conducted with the Nissan ASV-2 that the system detected the presence of a human body and prevented the vehicle from moving in that direction. These results provide confirmation that the prototype system is effective in helping to protect pedestrians in potential blind spots.

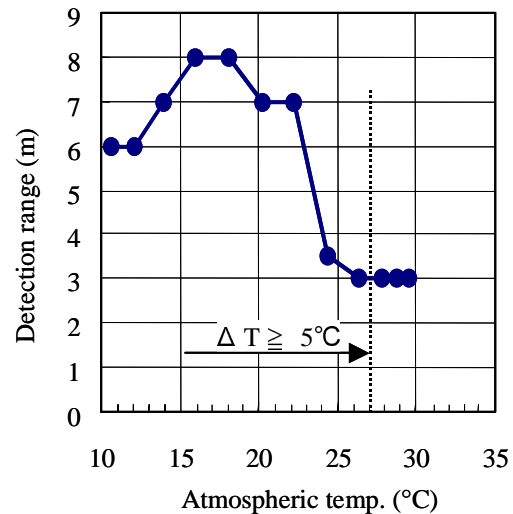


Fig. 14 Relationship between IR imager detection range and atmospheric temperature

REAR VIEW CAMERA WITH INTRARED IMAGE SENSORS

This system is a fusion of a visible rearview camera and the IR imaging sensor described above, enabling it to alert the driver to the presence of pedestrians in the rearward blind spot. The in-vehicle configuration of the system is shown in Fig. 15, and the positions of the devices are shown in Fig. 16.

An image processor combines the image signal from the visible camera with the detection results of two IR imaging sensors to produce a rearview image that is shown on a dashboard display screen. As shown in Fig. 15, the IR detection area achieved with the two IR imaging sensors is a trapezoid that measures 1.7 m along the width of the vehicle), 2.7 m on its long side and 2.1 m in distance from the vehicle. The long-side dimension with the IR imaging sensors and the distance along the ground are 2.7 m. A detected heat source is indicated on the screen by a red dot at the center of gravity of the detected region, and an audible warning is also given to alert the driver.

Based on the results shown in Fig. 14, the system is capable of detecting a human body in the entire detection area under a condition of $\Delta T = T_t - T_e \geq 3^\circ\text{C}$.

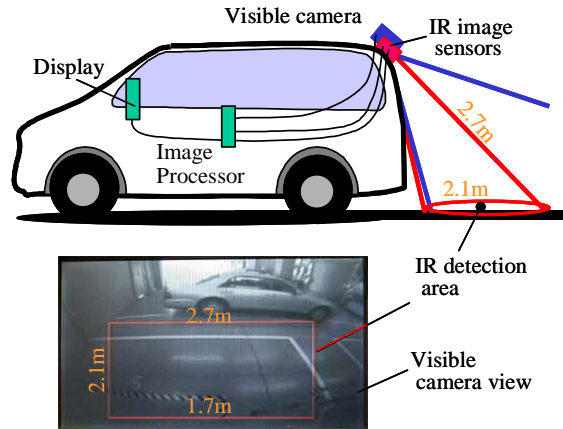


Fig. 15 System configuration

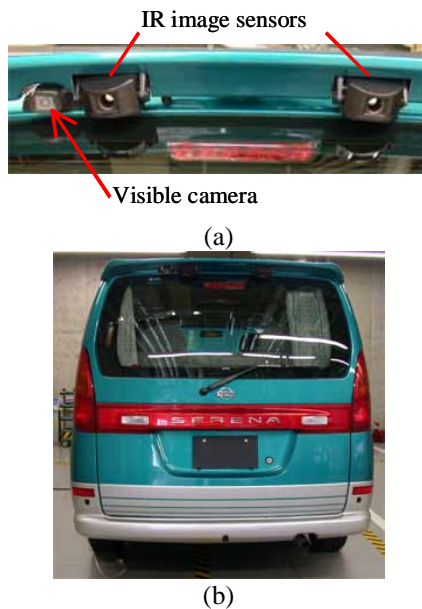


Fig. 16 IR camera system installed on Nissan ASV-2. (a) Enlarged view of installation positions and (b) entire rear-end

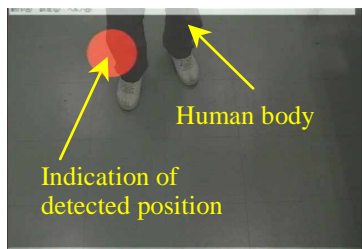


Fig. 17 Display screen showing detected human body

SUMMARY

The characteristics of IR radiation emitted by the human body were investigated by measuring the dependence of the facial surface temperature on the atmospheric temperature and solar radiation. The results made it clear that the facial surface temperature shows little change under a condition of a light wind.

A 48 x 32 element thermoelectric IR imaging sensor was developed that has the potential for a low cost. This sensor was used to develop a prototype blind spot pedestrian warning system that was incorporated in the Nissan ASV-2. In addition, it was also used to develop a prototype rearview camera system with IR detection capability.

The human body detection range is influenced by the background temperature and is 3 m under a condition of a temperature difference $\Delta T = 3^{\circ}\text{C}$. This detection range may be is effective for detecting the presence of pedestrians in potential blind spots around a vehicle, however research work in this area is continuing.

In future research work, it will be necessary to enhance the sensitivity of the IR imaging sensor so that it functions more effectively under various environmental conditions and to improve the weatherability of the optical system.

REFERENCES

- [1] C. Hanson, "Uncooled thermal imaging at Texas Instruments", SPIE, Vol. 1689, pp. 330-339, 1993.
- [2] R. A. Wood, C. J. Han, and P. W. Kruse, "Integrated uncooled IR detector imaging arrays", Proceedings of the IEEE Solid State Sensor and Actuator Workshop, pp. 132-135, 1992.
- [3] T. Kanno, and M. Saga, "Uncooled infrared focal plane array having 128 x 128 thermopile detector elements", SPIE, Vol. 2269, 1994.
- [4] M. Hirota, S. Morita, "Infrared sensor with precisely patterned Au-black absorption layer", SPIE, Vol. 3436, pp. 623-634, 1998.
- [5] M. Hirota, Y. Nakajima, M. Saito, F. Satou, and M. Uchiyama, "120x90 element thermopile array fabricated with CMOS technology", SPIE, Vol.4820, pp.239-249, 2002.

[6] M. Hirota, M. Saito, S. Morita, and H. Fukuhara, "Nighttime Pedestrian Monitoring System and Thermal Infrared Technology", JIDOSHA GIJUTSU, Vol. 50, No. 11, pp. 58-63, November 1996 (in Japanese).